0026-895X/06/6902-452–461$20.00
MOLECULAR PHARMACOLOGY
Vol. 69, No. 2
17566/3078686
Mol Pharmacol 69:452–461, 2006
Printed in U.S.A.

Probing the Reorganization of the Nicotinic Acetylcholine Receptor during Desensitization by Time-Resolved Covalent Labeling Using [^{3}H]AC5, a Photoactivatable Agonist

Alexandre Mourot,[1] Jordi Rodrigo,[2] Florence Kotzyba-Hibert, Sonia Bertrand, Daniel Bertrand, and Maurice Goeldner

Laboratoire de Chimie Bioorganique, Unité Mixte de Recherche (UMR) 7514 Centre National de la Recherche Scientifique (CNRS) (A.M., F.K.-H. M.G.) and Laboratoire de Bioinformatique du Médicament, UMR 7081 CNRS (J.R.), Faculté de Pharmacie, Université Louis Pasteur Strasbourg, Illkirch, France; and Département de Neurosciences, Centre Médical Universitaire, Faculté de Médecine, Geneva, Switzerland (S.B., D.B.)

Received August 2, 2005; accepted November 3, 2005

ABSTRACT

The structural reorganizations occurring on the nicotinic acetylcholine receptor (nAChR) during activation and subsequent desensitization have been investigated through time-resolved photoaffinity labeling using a photoactivatable nicotinic agonist. [^{3}H]AC5 is a photosensitive nicotinic probe with high affinity for the desensitized state of the *Torpedo marmorata* receptor (K_D = 5 nM) that displays full agonist activity on the *Torpedo californica* receptor expressed in oocytes (EC_{50} = 1.2 μM). Photoaffinity labeling of this receptor in the desensitized state showed a predominant specific labeling of γ and δ subunits, whereas the α subunit was barely labeled. Using a stopped-flow device combined with a flash photolysis quenching system, we investigated the covalent mapping of the subunits as a function of incubation time of the receptor with [^{3}H]AC5 (17 ms–1.25 h). During agonist-induced desensitization, specific labeling increased substantially, with similar time constants for γ and δ subunits (0.016 s^{-1}), whereas labeling of the α subunit remained relatively low. Therefore, the repartition of radioactivity shifted during desensitization from a weak but predominant labeling of the α and γ subunits toward a substantial labeling of γ and δ subunits. The observed time-dependent labeling pattern together with AC5 docking into a homology model of the *T. californica* nAChR suggest a subunit reorganization during agonist-induced desensitization, leading to a tightly packed arrangement that corresponds to a stable high affinity state for agonists.

The nicotinic acetylcholine receptor (nAChR) from *Torpedo* species electric organs and vertebrate neuromuscular junctions is a well characterized transmembrane allosteric heteromer composed of four proteins assembled into a pentameric structure $\alpha_2\beta\gamma\delta$. This receptor carries two acetylcholine (ACh) binding sites and contains the cation-selective channel-forming elements. nAChR from *Torpedo* species is a ligand-gated ion channel that undergoes allosteric transitions upon agonist binding: exposure to acetylcholine leads to a rapid (in milliseconds) opening of the channel, causing depolarization of the membrane, followed by a fast (milliseconds to seconds) and a slow (seconds to minutes) process of desensitization (Changeux and Edelstein, 1998).

The structure of the acetylcholine binding protein (AChBP), a homopentameric soluble homolog of the N-terminal extracellular domain of the nicotinic receptor, reveals the atomic arrangement of the amino acids that frame the ligand binding site of nicotinic receptors (Brejc et al., 2001; Celie et al., 2004). Moreover, refined cryoelectron microscopic analyses of two-dimensional crystalline arrays of nAChRs provided a definition of a three-dimensional structure of the closed nAChR approaching 4-Å resolution (Miyazawa et al., 2003; Unwin, 2005). Both structural analyses showed that the protein subunits display predominantly β-sheet folding

This work was supported by Association Française contre les Myopathies, by a fellowship (to A.M.), by CNRS, by the Université Louis Pasteur, and by a grant from the Swiss National Science Foundation (to D.B.).
[1] Current affiliation: Max Planck Institut für Biophysik, Frankfurt am Main, Germany.
[2] Current affiliation: Centre d'Études et de Recherche sur le Médicament de Normandie, Unité Propre de Recherche et de l'Enseignement Supérieur, Equipe d'Accueil 3915, Département de Modélisation Moléculaire, Université de Caen Basse-Normandie, Normandie, France.
Article, publication date, and citation information can be found at http://molpharm.aspetjournals.org.
doi:10.1124/mol.105.017566.

ABBREVIATIONS: nAChR, nicotinic acetylcholine receptor; ACh, acetylcholine; AChBP, acetylcholine binding protein; LBD, ligand-binding domain; Dns-C_6-Ch, dansyl-C_6-choline; EPB, epibatidine; CCh, carbamylcholine; DIFP, diisopropyl phosphofluoridate; dTC, *d*-tubocurarine; α-Bg-tx, α-bungarotoxin; PAGE, polyacrylamide gel electrophoresis; A, active; D, desensitized; R, resting.

in the ligand-binding domain (LBD) and α-helical folding in the pore domain, which lead us to address the key question of the structural reorganization of the receptor during gating and desensitization. Comparative analysis of the closed nAChR and AChBP structures (in complex with different agonists or antagonists) gave rise to tentative molecular models for the gating mechanism (Miyazawa et al., 2003; Celie et al., 2004, 2005; Hansen et al., 2005; Unwin, 2005). Despite these remarkable advances in the structural knowledge, the molecular description of the gating and desensitization phenomenon needs further clarification, notably by the use of time-resolved methods. Mutational and chemical investigations have thus been undertaken on the cys-loop family to elucidate the molecular motions occurring inside the ion pore (Horenstein et al., 2001; Wilson and Karlin, 2001), at the membrane-LBD interface (Absalom et al., 2003; Kash et al., 2003) as well as in the agonist binding site (Wagner and Czajkowski, 2001; Grutter et al., 2002, 2003; Gao et al., 2005). However, little effort has been spent to investigate the conformational reorganization occurring at the subunit interface during activation and subsequent desensitization.

Topographical mapping of residues constituting the ACh binding sites of *Torpedo* species nAChR was achieved by (photo)affinity labeling and site-directed mutagenesis, leading to the identification of three discontinuous domains on the α subunits (loops A, B, and C) with additional residues on the γ and δ subunits (binding segments D, E, F, and G). This seven binding-segment-domain model fits quite accurately with the three dimensional positioning of the homologous residues in AChBP (Brejc et al., 2001; Sine, 2002). Using time-resolved photolabeling methods, structural reorganization occurring at the acetylcholine binding domains upon desensitization were already studied at the molecular level, first with the antagonist [^{3}H]*p*-(*N*,*N*-dimethyl)aminobenzenediazonium fluoroborate (DDF) (Galzi et al., 1991), and more recently with the agonist [^{3}H](diazocyclohexadienoylpropyl)trimethylammonium (DCTA) (Grutter et al., 2002).

Dynamic photoaffinity labeling combines the power of photochemical covalent bond formation with rapid mixing techniques. A stopped-flow mixing device adapted with a photochemical quenching system was used to analyze the structural reorganization at the ACh binding site (Grutter et al., 2002). To extend this analysis to the αγ and αδ interfaces, we used [^{3}H]AC5, a molecule that was initially shown to be a potent photoactivatable agonist on mouse muscular nAChR (Chatrenet et al., 1992). AC5 (Scheme 1) is structurally related to the fluorescent agonist dansyl-C_6-choline (Dns-C_6-Ch), a probe that has been used to characterize the different states of the nicotinic receptor (Heidmann and Changeux, 1979) and more recently to determine binding characteristics of the αγ and αδ binding sites (Martinez et al., 2000; Song et al., 2003). Based on this structural analogy, it will be possible to correlate fluorescence analyses with dynamic photochemical mapping studies during the functioning of the receptor, probing in particular the αγ and αδ subunit interfaces.

In this article, we have established that AC5 possesses binding and activation properties analogous to ACh on the *Torpedo* species nAChR. Using both time-resolved photochemical and molecular modeling approaches, we have analyzed the reorganization of the *Torpedo marmorata* nAChR at the αγ and αδ subunit interfaces upon AC5-induced activation.

Materials and Methods

Reagents. AC5 and [^{3}H]AC5 (0.7–0,9 Ci/mmol after isotopic dilution) were synthesized and purified according to experimental conditions described previously (Mourot et al., 2002). Epibatidine (EPB) was synthesized as described elsewhere (Che et al., 2003). ACh, carbamylcholine (CCh), diisopropyl phosphofluoridate (DIFP), proadifen, decamethonium, and *d*-tubocurarine (dTC) were purchased from Sigma (St. Louis, MO), and complete mini EDTA-free protease inhibitor cocktail tablets were purchased from Roche GmbH (Mannheim, Germany).

nAChR-Rich Membrane Preparation. nAChR-rich membranes were isolated after alkali treatment from *T. marmorata* electric organs as described previously (Grutter et al., 2002). The final membrane suspension contains 3 to 4 nmol of ^{125}I-α-bungarotoxin (α-Bg-tx) binding sites per milligram of protein.

[^{3}H]AC5 Binding Assay. The equilibrium binding of [^{3}H]AC5 to nAChR rich membranes was measured in the dark at room temperature. The membranes (4 nM ^{125}I-α-Bg-tx binding sites) were equilibrated with 15 μM proadifen and 250 μM DIFP for 50 min in a buffer (10 mM NaP_i and 150 mM NaCl, pH 7.2) containing the protease inhibitor cocktail. Samples were then incubated for 30 min with different concentrations of [^{3}H]AC5 (1–100 nM), rapidly quenched by 2.5 ml of the same buffer, and filtered on GF-C glass fiber filters (Whatman, Maidstone, UK) saturated with 0.3% polyethylenimine. Nonspecific binding was determined in the presence of 100 μM CCh added 30 min before [^{3}H]AC5. Radioactivity associated with the filter was counted. Equilibrium binding data were fitted to a single-site model with a linear, nonspecific binding component with the equation $B(x) = [(B_{max} \times x)/(K_{eq} + x)]^{n_H} + b \times x$, where $B(x)$ is the [^{3}H]AC5 bound at a free concentration x, B_{max} is the concentration of [^{3}H]AC5 binding sites, K_{eq} is the dissociation constant, n_H is the Hill number, and b is the slope for nonspecific binding.

Electrophysiology. pMXT plasmids encoding the *Torpedo californica* wild-type α, γ, and δ subunits and pSP64 plasmid encoding the β subunit were a gift from Jonathan B. Cohen (Harvard Medical School, Boston, MA). cDNAs were linearized with either XbaI (pMXT plasmids) or FspI (pSP64 plasmid) and transcribed in vitro using the SP6 mMessage mMachine kit (Ambion, Austin, TX). Stage V to VI oocytes were prepared using standard techniques (Bertrand et al.,

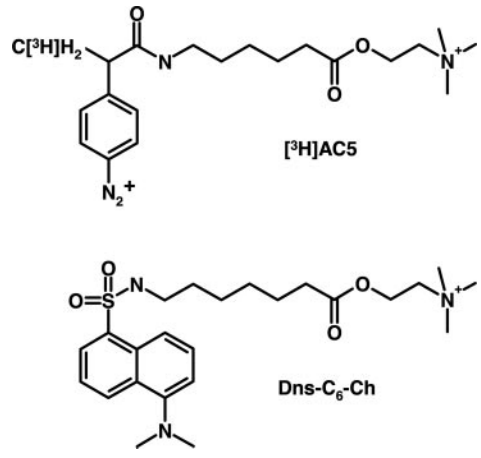

Scheme 1. Chemical structures of two structurally related nicotinic agonist probes: the photosensitive tritiated [^{3}H]AC5 and the fluorescent Dns-C_6-Ch. Both molecules carry an acyl choline moiety attached through a similar spacer either to the fluorescent dansyl chromophore (Dns-C_6-Ch) or to the photosensitive aromatic diazonium salt (AC5). AC5 = (2-trimethylammonium)-ethyl-6-*N*-[*N*′-(methyl)-*para*-diazonium-phenylurea]-hexanoate trifluoro-acetate.

1991) and injected with *T. californica* cRNAs. A total of 20 ng of cRNA that contained a mixture of α, β, γ, and δ subunits in equal amounts was injected into the oocytes 2 to 3 days before the experiments. Oocytes were superfused during the entire experiment with a solution containing 82.5 mM NaCl, 2.5 mM KCl, 5 mM HEPES, 2.5 mM $CaCl_2$, and 1 mM $MgCl_2$ (pH 7.4, adjusted with NaOH). Atropine (1 μM) was added to prevent activation of endogenous muscarinic receptors. Cells were held at -100 mV throughout the experiment using a dual electrode voltage clamp (GeneClamp; Molecular Devices, Sunnyvale, CA). Drugs were applied in perfusion using computer-driven electromagnetic valves. ACh- and AC5-evoked currents were recorded in response to test pulses (3 s) applied once every 2 min in the dark. Dose-response curves were obtained by plotting the peak of the evoked current as a function of the logarithm of the agonist concentration. Fits were done using the empirical Hill equation: $y = I_{max}/[1 + (EC_{50}/x)^{n_H}]$, where y is the peak of the evoked currents, EC_{50} is the half-activation in micromolar, x is the agonist concentration in micromolar, and n_H is the Hill coefficient.

Photolabeling of nAChR at Equilibrium. nAChR-rich membranes (200 pmol, 400 nM) were equilibrated with 15 μM proadifen and 250 μM DIFP for 45 min at 4°C in 500 μl of a buffer (10 mM NaP_i and 150 mM NaCl, pH 7.2) containing protease inhibitor cocktail. [^{3}H]AC5 (500 nM) was then incubated for 15 min with the membranes before photolysis. Protection experiments were carried out with preaddition (30 min at 4°C) of either 100 μM CCh or various concentration of CCh, dTC, EPB or decamethonium. Samples were then irradiated for 15 min at 385 nm (monochromator; HORIBA Jobin-Yvon SAS, Longjumeau, France), 40 μV, 10°C. In such irradiation conditions, the half-life of AC5 was found to be around 4 min (not shown). After irradiation, photolabeled nAChRs were recovered after one-step centrifugation (11,000*g*, 30 min, 4°C) and pellets were solubilized for 30 min at 30°C in the Laemmli sample buffer. The samples were loaded onto an 8% SDS-PAGE, and radioactivity incorporated in each subunit was quantified as described previously by scintillation counting of excised gel pieces (Langenbuch-Cachat et al., 1988).

Time-Resolved Photolabeling. Time-resolved photolabeling was performed at 10°C in the rapid mixing system (Fig. 3A) using the same buffer as for photolabeling at equilibrium. A 1- to 2-ml/s flow was chosen, which corresponds to an irradiation time of less than 30 ms. To achieve flash photolysis of AC5, we used the broadband of the 1000-W, high-pressure xenon/mercury lamp (Osram) and, under these conditions, more than 90% of the AC5 could be photolyzed in 15 ms (not shown). Different experimental conditions were realized, as follows

For short mixing times (< 1 min), nAChR-rich membranes (syringe 1, 650 nM concentration in delay loop 1) were first incubated with ACh (syringe 2, 600 nM final concentration in loop 1) for 450 ms to saturate approximately 20% of pre-existing high-affinity binding sites in the absence of any effector molecule (Galzi et al., 1991). This solution (325 nM final concentration of ACh binding sites in delay loop 2) was mixed with [^{3}H]AC5 (syringe 3, 500 nM final concentration in delay loop 2) for a chosen mixing time and irradiated. Protection experiments were carried out by mixing the membranes (syringe 1, 650 nM concentration in delay loop 1) 450 ms with CCh (syringe 2, 500 μM final concentration in delay loop 1) before [^{3}H]AC5 incubation (delay loop 2).

For long mixing times (>1 min), nAChR-rich membranes (325 nM) were mixed with [^{3}H]AC5 (500 nM) out of the stopped-flow apparatus, incubated for a chosen mixing time in the dark at 10°C, and then loaded into syringe 3 for irradiation. Protection experiments were carried out by coincubation with CCh (500 μM).

For photolabeling of the nAChR preincubated with proadifen. The membranes (1.3 μM binding site) were first incubated 45 min with 15 μM proadifen at 10°C before loading into the syringe 1. Syringe 2 was filled with buffer, and nAChRs were first diluted (650 nM delay loop 1) before being mixed 125 ms with [^{3}H]AC5 (syringe 3, 500 nM in delay loop 2) and irradiated.

The samples were then collected in the collection syringe, centrifuged (11,000*g*, 30 min, 4°C), solubilized for 30 min in Laemmli buffer, and loaded onto an 8% SDS-PAGE. The quantification of the radioactivity was performed as described above for photolabeling at equilibrium.

Homology Modeling and Docking Simulations of the *T. californica* nAChR. The nAChR subunit alignment presented by Brejc et al. (2001) was used, and the AChBP structure was examined to ensure that insertions and deletions occurred within exposed flexible fragments. The Biopolymer module of Sybyl (ver. 7.0; Tripos, St. Louis, MO) was used to mutate the nAChR sequences into the AChBP structure. Because the most important requirement in homology modeling is a correct alignment between the sequence to be modeled with that of the template structure, we compared the alignment proposed by Brejc et al. (2001) with other alignments that have been published recently (Le Novere et al., 2002; Molles et al., 2002; Schapira et al., 2002). All multiple alignments show a good overall conservation within the secondary structure and the different loops, except for the F segment. Compared with the primary structure of the AChBP, the nAChR α-subunit of *T. californica* contains insertion in two regions within the ACh binding site. Although segment C in all neuronal nAChR α-subunits align well with the AChBP, the *T. californica* and skeletal muscle α-subunits contain a single residue insertion between αCys192 and αTyr198. We designated αAsp195 as the inserted residue. The other α-subunit insertion in the vicinity of the binding site was αAla96 in segment A. The only portion of nAChR subunit primary structure that did not allow a straightforward substitution was the poorly aligned sequence encompassing the amino acids of binding site segment F. This region of primary structure required insertions of 9, 7, and 11 amino acids in the β, γ, and δ subunits, respectively, in the segment region between β8 and β9 β-strands. Lacking additional guidelines, we positioned these insertions (β164–172, γ164–170, and δ166–176) in external loops to preserve the structure of the adjacent regions that were homologous to the AChBP sequence.

To prepare the protein structure for energetically minimization and docking experiments, partial atomic charges were assigned to each atom of the protein using the restrained electrostatic potential charge model of the AMBER 8 (Case et al., 2004) program. Because AC5 structure was not solved, the molecule was built using the program ChemDraw and translated to three dimensions using the Concord program. A short minimization was performed in Sybyl and the molecule was protonated subsequently. The whole structure was energy-minimized using the program AMBER8 (2000 steps of steepest descent + conjugate gradient) and we should remark that both insertions in the C and A loops were well tolerated. Then, we used the docking program GOLD (genetic optimization for ligand docking; ver. 2.1) (Jones et al., 1997) to dock AC5 to both α-γ and α-δ binding site. GOLD is an automated ligand-docking program that uses a genetic algorithm to explore the full range of ligand conformational flexibility.

AC5 Docking into the AChBP Based on the Structure of an AChBP-Conotoxin Complex. The AC5 molecule was docked into the crystal structure of AChBP from *Aplysia californica* in complex with an α-conotoxin (Protein Data Bank entry 2br8) (Celie et al., 2005). The same procedure as for *T. californica* nAChR receptor was used to prepare the protein structure for energy minimization and docking experiments. After removing the α-conotoxin, the AC5 was placed in the cavity. The whole structure was energy-minimized using the program AMBER8 (2000 steps of steepest descent + conjugate gradient). Again, we used the docking program GOLD to dock AC5 into the cavity. Distance constraints (1.5–3.5 Å) were set between the nitrogen atom of the quaternary ammonium of AC5 and the centroid of the benzyl part of the Trp145.

Results

Biochemical Properties of AC5. Previous competition experiments against ^{125}I-α-Bg-tx initial binding rate have shown that nonlabeled AC5 binds with high affinity (9 nM) to the ACh binding site in the desensitized state (Chatrenet et al., 1992). Here, we extend the study by measuring the equilibrium binding of [^{3}H]AC5 on nAChR-rich membranes, in the presence of proadifen (15 μM), conditions in which the receptor is mainly in the high-affinity desensitized state (Heidmann and Changeux, 1979). The experiments were performed in the dark, in the presence of 250 μM DIFP. This DIFP concentration was sufficient for complete inhibition of AChE activity, thus avoiding any [^{3}H]AC5 degradation (data not shown). Figure 1A shows that non specific binding (with saturating CCh concentration) was a linear function of [^{3}H]AC5 concentration, at least up to 100 nM. The specific binding fits well with a simple hyperbolic function characterized by K_d = 5 nM and the concentration of [^{3}H]AC5 binding sites (3.5 nM) was near the concentration of ^{125}I-α-Bg-tx binding sites (4 nM), establishing that AC5 binds with both ACh binding sites. The Hill number near 1 is characteristic of a single class of binding sites. Dissociation constant of [^{3}H]AC5 for the high-affinity desensitized D state is thus very close to the K_d measured for [^{3}H]ACh [7 nM (Neubig and Cohen, 1979)] and for Dns-C_6-Ch [9 nM for the αγ and 3 nM for the αδ sites (Song et al., 2003)]. Furthermore, it has been shown that the AC5 derivative lacking the choline moiety is a very weak ligand of the ACh binding sites (Chatrenet et al., 1992). Together, these results show that the high affinity of the probe for the receptor is governed mainly by specific interactions with the acetylcholine moiety of the molecule.

Functional Properties of AC5. To assess the capacity of AC5 to evoke currents on *Torpedo* species receptors, expression experiments were designed using *Xenopus laevis* oocytes. As shown in Fig. 1B, AC5 evoked robust currents that display maximal amplitude comparable with ACh. Time course of the evoked responses (Fig. 1B, inset) revealed no detectable difference in the time course of ACh-evoked currents (data not shown). Plot of the peak current evoked by growing concentrations of AC5 and ACh as a function of the logarithm of the agonist concentration yielded typical dose-response curves, represented in Fig. 1B. Continuous lines through the data points are the best fit obtained with the Hill equation. Comparison of the concentration required to activate half of the maximal evoked current (EC_{50}) between ACh and AC5 revealed that the latter is a slightly more potent agonist than ACh. The slightly smaller amplitude observed in response to AC5 compared with ACh was consistent but hardly significant. Together, these results demonstrate that AC5 is a potent agonist of the *T. californica* muscle nAChR.

Photoaffinity Labeling on the D State. In a first series of experiments, photolabeling studies were carried out on nAChR-rich membranes (400 nM ^{125}I-α-Bg-tx binding sites) in the presence of the desensitizing noncompetitive antagonist proadifen (Heidmann and Changeux, 1979; Galzi et al., 1991) and with the esterase inhibitor DIFP. The concentration of [^{3}H]AC5 used (500 nM) was sufficient to occupy, at equilibrium in the dark, at least 98% of the agonist binding sites. After 15 min of photolysis, the pattern of incorporation was assessed by SDS-PAGE 8%, by liquid scintillation counting of the bands excised from the gel. Figure 2A shows that UV irradiation (at 385 nm) of the complex resulted in a

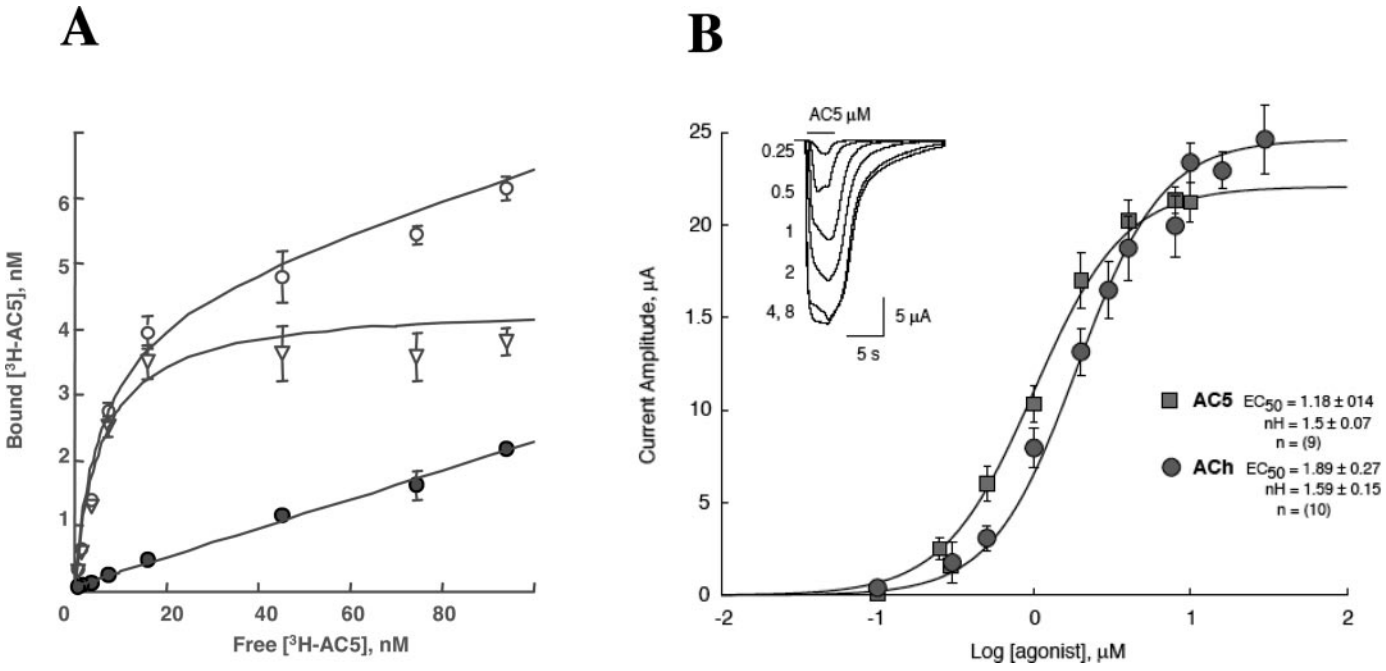

Fig. 1. Pharmacological and physiological properties of AC5. A, saturation experiment with [^{3}H]AC5 on desensitized nAChR. nAChR-rich membranes (4 nM ^{125}I-α-Bg-tx binding sites) were equilibrated with 15 μM proadifen and 250 μM DIFP for 50 min, incubated for 30 min with different concentrations of [^{3}H]AC5 (1–100 nM), and then rapidly filtered. Nonspecific binding (●) was determined in the presence of 100 μM CCh added 30 min before [^{3}H]AC5. Specific binding (▽) was determined by the difference between total binding (○) and nonspecific binding (●). Bars indicate the S.E.M. for three independent experiments. B, electrophysiology experiment. Dose-response relations and fits to the Hill equation for wild-type *T. californica* nAChR expressed in oocytes by using either AC5 or ACh. Bars indicate the S.E.M. for n = 9 cells in ACh and n = 10 cells in AC5. Inset, typical AC5-evoked currents recorded in an oocyte in response to a series of test pulses with different concentrations are superimposed. The timing of the AC5 application is indicated by the bar.

specific covalent incorporation of radioactivity mainly in the γ (52–57% of the specific incorporation, 70–80% protection by 100 μM CCh) and δ subunits (40–45% of the specific incorporation, 65–75% protection by 100 μM CCh). The labeling of the α subunit was very low and only partially protectable (1–3% of the specific incorporation, 15–25% protection by 100 μM CCh). The negligible specific incorporation found at the level of the β subunit most probably arose from partial proteolysis of the γ subunit (data not shown) rather than direct labeling of the β subunit. In such experimental conditions, [^{3}H]AC5 is incorporated in ~7% of the ACh binding sites. In the absence of light, no detectable specific labeling was observed (data not shown).

The structural dissimilarity between the γ and δ subunits generates a pharmacological nonequivalence between the two agonist binding sites. We thus decided to investigate the inhibition of photolabeling in both sites using different competitors at various concentrations (1–100 μM): three agonists (CCh, EPB, and decamethonium) and one competitive antagonist (dTC). Figure 2B shows that CCh protects the labeling of the γ and δ subunits in a similar fashion, which is in full agreement with the identical affinity of CCh for both binding sites. Protection of labeling, however, is much more efficient on the γ subunit compared with the δ subunit using EPB, dTC, or decamethonium as a competitive ligand. These protection patterns clearly show that $\alpha\gamma$ constitutes the high-affinity binding site for dTC and EPB, as previously pointed out by photolabeling (Pedersen and Cohen, 1990) and fluorescence with Dns-C_6-Ch (Song et al., 2003). To our knowledge, binding selectivity of decamethonium to the $\alpha\gamma$ binding site has not been shown before.

Time-Resolved Photoaffinity Labeling. To investigate the [^{3}H]AC5 incorporation pattern on transient states of the receptor, we have used the previously described stopped-flow apparatus connected to a photochemical quenching system (Fig. 3A) (Grutter et al., 2002). We analyzed the incorporation of [^{3}H]AC5 on nAChR rich membranes as a function of mixing time in the dark, which ranged from 17 ms to 1.25 h. In the absence of any effectors, the nAChR of *T. marmorata* is in equilibrium between the low-affinity resting state (R) and the high-affinity desensitized state (D). According to fluorescence experiments with Dns-C_6-Ch, predesensitized receptors represent approximately 20% of nAChR population (Heidmann and Changeux, 1979). For short incubation times (<1 min), we thus rapidly (450 ms) mixed the membranes with a low concentration (600 nM) of ACh to occupy the preexisting high-affinity sites, thus avoiding any labeling of the nAChR in the D state. Protection experiments were carried out by rapidly mixing (450 ms) CCh (500 μM) with the membranes before [^{3}H]AC5 incubation. For longer incubation times (>1 min), [^{3}H]AC5 was directly mixed with nAChR-rich membranes without using the stopped-flow apparatus, with or without CCh (500 μM).

For mixing times shorter than 1 s, the specific radioactivity incorporation pattern remained steady, very low, and was mainly associated with the α and γ subunits and, to a smaller extent, with the δ subunit (Fig. 3, B and C). Labeling is protectable (30–70%) on all three subunits by 500 μM CCh. Less than 1% (0.4–1%) of the ACh binding sites are specifically labeled with such short mixing times.

For mixing times longer than 300 s, the radioactivity incorporation pattern was also constant but associated mainly with the γ and δ subunits and in a minor way with the α subunit (Fig. 3, B and C). Under these conditions, 5.4 to 7.4% of the ACh binding sites are specifically labeled by [^{3}H]AC5. Both efficiency and repartition of specific labeling were very

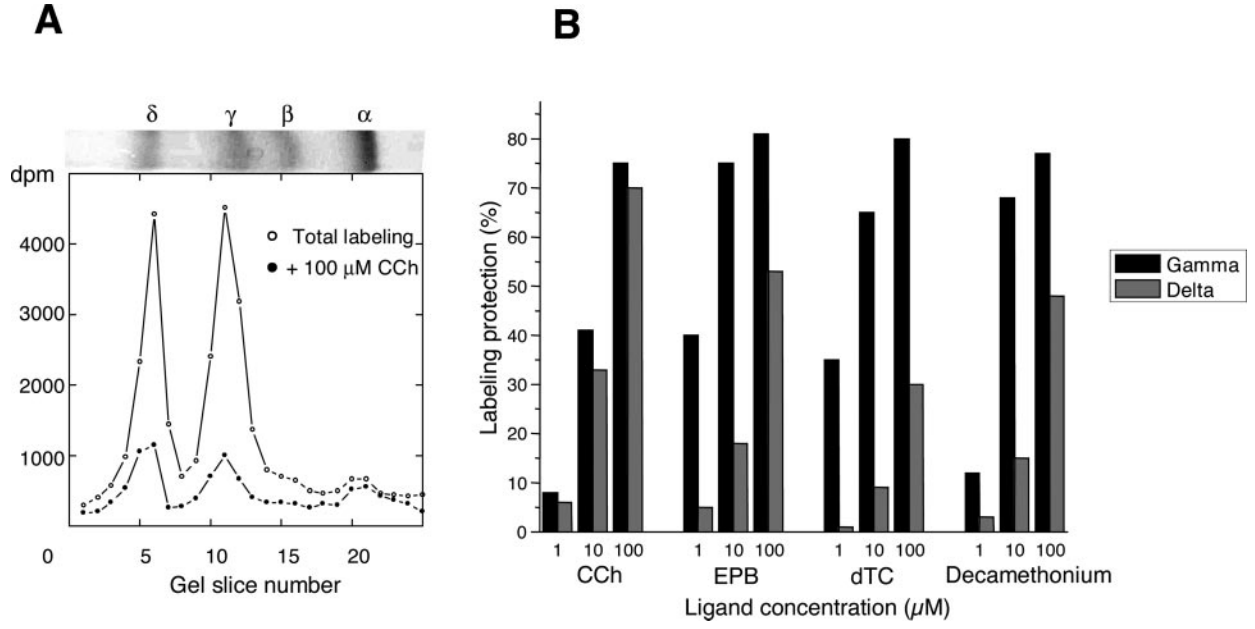

Fig. 2. Photo-incorporation of [^{3}H]AC5 into the desensitized *T. californica* nAChR. A, [^{3}H]AC5 incorporation pattern on a 8% SDS-PAGE. nAChR-rich membranes (200 pmol) were irradiated (385 nm, 15 min) with 500 nM [^{3}H]AC5, with or without CCh (100 μM), under conditions in which the receptor was, to a large extent, desensitized (preincubation 50 min with proadifen 15 μM). Distribution of the radioactivity was measured after gel slicing, digestion, and counting. The position of the nAChR subunits are indicated above the gel. B, effect of CCh, EPB, dTC, and decamethonium concentration on the photoincorporation of [^{3}H]AC5 into nAChR-rich membranes. Desensitized nAChRs (200 pmol) were irradiated with 500 nM [^{3}H]AC5, with or without preincubation with different concentrations (1, 10, and 100 μM) of CCh, EPB, dTC, or decamethonium. The distribution of the radioactivity in the γ and δ subunits was measured, and the protection of labeling was calculated by comparing the extent of labeling with and without protector. This figure depicts one representative experiment.

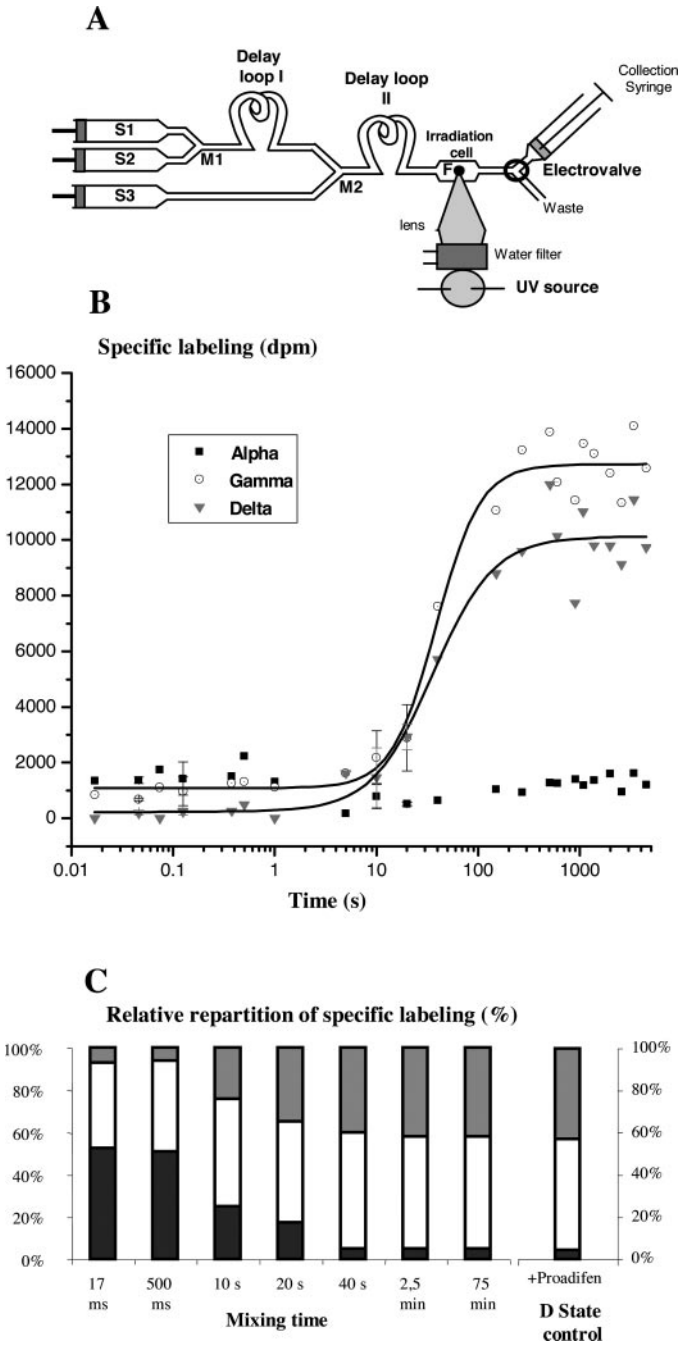

Fig. 3. Time-resolved labeling with [^{3}H]AC5. A, schematic representation of the rapid-mixing device used for time-resolved photolabeling. The different reactants were loaded into three syringes, rapidly mixed in chambers M1 and M2, and delayed in loops 1 and 2 before being irradiated with UV light in the quartz cell. The incident light beam was focused on the quartz cell (31 μl) to obtain a maximum illumination. A 1–2 ml/s flow rate was selected, which corresponds to an irradiation time between 15 and 30 ms. Samples were then collected in the collection syringe for SDS-PAGE analyses. B, specific incorporation of radioactivity into the α, γ, and δ subunits as a function of the mixing time. SDS-PAGE analysis of [^{3}H]AC5 (500 nM) photoincorporation as a function of the mixing time in the dark with nAChR-rich (325 nM) membranes. Nonspecific labeling was carried out with preaddition of CCh (500 μM). Distribution of the radioactivity into each subunit was measured after gel slicing, digestion, and counting. For short mixing times (<1 s), specific labeling is mainly associated with the α (43–52% of the specific labeling) and γ subunits (40–48% of the specific labeling) and to a smaller extent with the δ subunit (0–12%). Labeling is protectable (30–70%) on all three subunits by CCh. Less than 1% (0.4–1%) of the ACh binding sites are specifically labeled with such short mixing times. For mixing times longer than 300 s, close to those observed for the nAChR desensitized by proadifen and photolabeled at equilibrium (Fig. 2A). However, to compare the labeling results in identical irradiation conditions, we photolabeled nAChRs desensitized by proadifen using the rapid-mixing device. We found no significant difference between these two experimental conditions, with respect to the labeling pattern (Fig. 3C) or the photolabeling efficiency (5–7%).

For intermediate mixing times (1–300 s), a progressive enhancement of the photolabeling yield was observed, concomitantly on the δ and γ subunits, whereas labeling of the α subunit remains low (Fig. 3B). Both γ and δ labeling follow a monoexponential increase, and the half-life of this process can be estimated to be ~40 s. Specific labeling of the α subunit seems to decrease between 1 and 40 s, but the amount of alkylated α subunits remains too low to allow any reliable fitting analysis. Therefore, the relative repartition of specific labeling (Fig. 3C) indicates a progressive evolution going from a predominant labeling of the α and γ subunits (short mixing times) toward the γ and δ subunits (long mixing times). Finally, no detectable specific labeling was observed in the absence of light (data not shown).

Homology Modeling. It has been suggested that the tight structure of AChBP corresponds to a high-affinity open or desensitized state of the nAChR (Le Novere et al., 2002; Unwin et al., 2002). To confirm this hypothesis, and to analyze our photolabeling patterns more in detail, we built a homology model of *T. californica* nAChR based on AChBP structure (Protein Data Bank code 1I9B) (Brejc et al., 2001). We have used the approach of comparative modeling based on a template of known structure. This is the best approach available when a homolog of the target is known. However, it is important to keep in mind the limitations inherent to a modeling process built on a sequence identity inferior to 30% between the template and the target. AChBP shares between 20 and 28% sequence identity with the LBD of nAChRs and is thus the established model for the extracellular domain of these receptors. Until now, several homology models have been generated to analyze receptor-ligand interactions with nicotinic receptors (Le Novere et al., 2002; Molles et al., 2002; Schapira et al., 2002).

The automated docking of AC5 in both ligand-binding pockets led to a positioning of the ligand consistent with labeling experiments and with recent AChBP structure in complex with CCh (Celie et al., 2004). AC5 docked in a similar way in the α-γ and α-δ binding-sites even though the score value of the docking program GOLD for AC5 was higher in α-γ than α-δ. As has been shown, the quaternary

the radioactivity incorporation pattern is associated with the γ (50–56% of the specific labeling, 80–90% protection by 500 μM CCh) and δ subunits (37–46% of the specific labeling, 80–90% protection by 500 μM CCh) and in a minor way with the α subunit (4–8% of the specific labeling, 30–50% protection by 500 μM CCh). Under these conditions, 5.4 to 7.4% of the ACh binding sites are specifically labeled by [^{3}H]AC5. [^{3}H]AC5-specific incorporations into the γ and δ subunits can be analyzed with the monoexponential equation: $L(t) = L_{max}\,[1 - \exp(-k_{app} \times t)] + L_{min}$, where L_{max} and L_{min} are the maximum and minimum of the specific labeling, respectively, k_{app} is the pseudo–first-order time constant ($k_{app} = \ln 2/t_{1/2}$), and t is the mixing time in the dark. (n = 1–3). C, relative repartition of specific labeling (Lr) as a function of the mixing time. Specific labeling on the α, γ, and δ subunits is normalized to 100%: $Lr_{tot} = Lr_\alpha$ (black) + Lr_γ (white) + Lr_δ (gray) = 100%. D-state control represents the proadifen predesensitized nAChRs photolabeled via the rapid mixing device.

ammonium of acetylcholine makes a cation-π interaction with an αTrp (for review, see Lester et al., 2004). Indeed, in our model, the quaternary ammonium makes a cation-π interaction with αTrp149 (Fig. 4C), whereas the rest of the molecule is oriented toward an open space that is the probable route for ligand access (Brejc et al., 2001) (Fig. 4, A and B). The photoreactive aryl diazonium of AC5 (situated around 14 Å from the trimethylammonium moiety) is located out of the agonist binding site, near the complementary (i.e., the γ or δ) subunit. To validate our model, we also docked the acetylcholine into the α-γ binding site and found the interactions previously proposed by Le Novere et al. (2002) (data not shown). Comparing the docking positions of AC5 with ACh, we found that the positioning of the quaternary ammonium groups were only 1 Å apart from one another. Segment F residues are more distantly related to the core structure of the agonist binding site and according to our docking results, we believe that the predicted position of these residues do not have a significant influence on AC5 binding.

AC5 Docking into a Resting State-Like AChBP. α-Conotoxins are peptide toxins from cone snail venoms and are known to competitively inhibit nAChRs. They are believed to stabilize the inactive resting state (R) of the nAChRs. The structure of an AChBP in complex with an α-conotoxin PnIA variant was recently solved; it shows an opening of the C loop belonging to the ACh binding site and a small reorientation of the subunits with respect to one another (Celie et al., 2005). Because this structure of AChBP provides a model for the resting state conformation of the nAChR, we decided to dock the AC5 molecule into this structure.

A first attempt to dock the AC5 molecule into AChBP produced a high diversity of docking positions. Because the cavity volume in the AChBP from *A. californica* was bigger than in the *T. californica* nAChR model (989 versus 864 Å, respectively) and because of AC5's high flexibility and expected low affinity for this resting-state like structure (Heidmann and Changeux, 1979), we had to set a distance constraint between the probe and residues of the binding pocket. The Trp145 (equivalent αTrp149 in *T. californica*) and the quaternary ammonium of AC5 were good candidates for this distance constraint, in that the cation-π interaction is known to be a major ACh-nAChR interaction (Lester et al., 2004). Docking results confirmed the expected high flexibility of the AC5 molecule in the AChBP cavity, compared with the *T. californica* nAChR model. In the *T. californica* nAChR model, AC5 mobility was restricted by a narrow open space; however, in the AChBP structure, various docking positions are observed. Because of distance constraints, the quaternary ammonium is kept fixed in front of the Trp145. The photoactivatable aryl diazonium can be placed in multiple positions, from the C loop of the principal subunit up to the subunit interface in the upper part of the ACh binding site (Fig. 5, A and B)

Discussion

In this study, we used [^{3}H]AC5, a previously described nicotinic photoactivatable agonist whose structure combines an acyl choline moiety with an aromatic diazonium salt separated by a flexible spacer (Chatrenet et al., 1992). We showed that, in the dark, this molecule displays pharmacological and physiological features very similar to those of both the natural neurotransmitter ACh and the structurally related fluorescent probe Dns-C_6-Ch. Indeed, AC5 acts as a full agonist on *T. californica* receptors expressed in oocytes, displaying evoked currents with similar potency and time course as ACh. This photoprobe is thus a valid model of the natural agonist ACh, which prompted us to investigate the agonist-induced reorganization of the nAChR at the subunit interfaces.

Upon irradiation, [^{3}H]AC5 incorporates into the α, γ, and δ subunits of the desensitized nAChR, in a protectable (CCh-sensitive) fashion, with a mean ratio of 3:54:43, respectively. Although the agonist binding sites are located at the interface of two subunits, the complementary subunits (γ and δ) are labeled considerably more than the principal component (α). These labeling results are fully supported by AC5 docking into the ACh binding sites of our homology model of *T. californica* LBD, orienting the photoactivatable part of the AC5 molecule toward the γ and δ subunits (Fig. 4). Although we did not identify the residues labeled by [^{3}H]AC5 in the desensitized D state, several elements allow us to be confident with our docking model. First, the trimethylammonium of AC5 is located in the aromatic box of the ligand binding pocket and establishes cation-π interactions mainly with

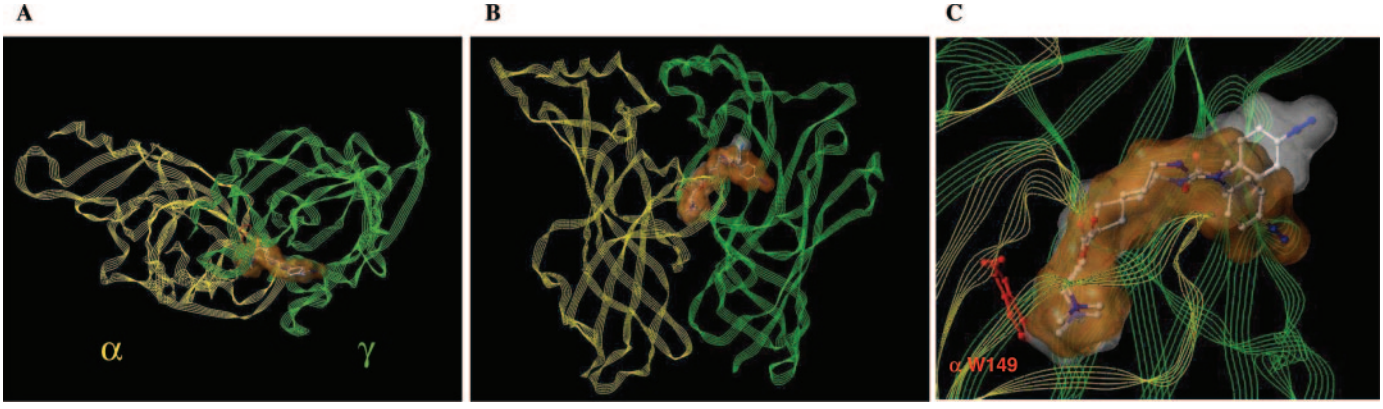

Fig. 4. AC5 probe orientation into the $\alpha\gamma$ binding site of the *T. californica* nAChR. A homology model of the *T. californica* nAChR was constructed from the crystal structure of AChBP (Brejc et al., 2001). Top (A) and side (B) views of the $\alpha\gamma$ dimer (ribbon representation), showing two docking results of AC5 molecule (ball and stick representation, with molecular surface in orange and blue), representative of maximal liberty of the probe in this site. C, frontal view of the cation-π interaction between the side chain of α Trp 149 (represented in red) and the trimethylammonium group of AC5.

Trp149, in agreement with numerous biophysical and structural data (Celie et al., 2004; Lester et al., 2004). Second, the acetylcholine part of AC5 has an orientation similar to that of the CCh molecule in the crystallographic structure of AChBP (Celie et al., 2004), and both molecules display agonist properties on *Torpedo* species nAChR. Third, the likely access route of agonists forms a narrow channel that forces the flexible AC5 molecule to adopt a particular conformation. Finally, two photoactivatable antagonists displaying structure similarities with AC5 also orient their photosensitive moiety toward the γ and δ subunits (Wang et al., 2000; Chiara et al., 2003). This photolabeling pattern on the D state thus fits very well with the hypothesis that AChBP tight structure corresponds to the high-affinity desensitized state of the nAChR (Le Novere et al., 2002), although we cannot exclude that it represents the high-affinity active state (Unwin et al., 2002).

[^{3}H]AC5 photoincorporates specifically in 5 to 7% of the ACh binding sites of the D-state nAChR. This photoincorporation yield is rather low compared with other aryl diazonium probes (Langenbuch-Cachat et al., 1988). However, this is not surprising because AC5 docking in the *T. californica* LBD model (Fig. 4) suggests a localization of the photoactivatable moiety outside of the protein core. Proximity of water molecules could therefore quench the photogenerated species, explaining the low incorporation efficiency observed.

The specific incorporation of radioactivity is always slightly higher for the $\alpha\gamma$ (6–7%) than for the $\alpha\delta$ binding sites (5–6%), even with saturating concentration of [^{3}H]AC5 (data not shown). [^{3}H](diazocyclohexadienoylpropyl)trimethylammonium, [^{3}H]nicotine, and [^{3}H]TDBzCh also react noticeably and predominantly within the $\alpha\gamma$ binding site (Middleton and Cohen, 1991; Grutter et al., 2002; Chiara et al., 2003). All these ligands display equal affinities for both binding sites; therefore, the photoincorporation selectivity must reflect a difference in the efficiency of covalent bond formation. As previously proposed, water quenching of the photogenerated species explains such an observation, thus suggesting a more hydrophobic and/or closed $\alpha\gamma$ binding site in the desensitized receptor (Chiara et al., 2003). A more compact $\alpha\gamma$ binding site has already been proposed based on fluorescence experiments with Dns-C_6-Ch (Martinez et al., 2000). The $\alpha\gamma$ binding site is clearly the high-affinity binding site for several nicotinic agonists (EPB, decamethonium) and antagonists (dTC), as confirmed by our photolabeling protection experiments (Fig. 2B) (Pedersen and Cohen, 1990; Song et al., 2003).

[^{3}H]AC5 photoincorporation patterns and efficiencies are highly dependent on the mixing time between the probe and the receptor in the dark (Fig. 3, B and C). Because the incorporation is protectable by CCh, it occurs specifically within both agonist binding sites. For mixing times longer than 300 s, nAChRs are most probably fully desensitized, because 1) both labeling patterns and efficiencies are comparable with those observed for nAChR desensitized with the NCB proadifen (at equilibrium and via the stopped-flow apparatus), and 2) it has been shown that most of the receptors were desensitized after 400 s incubation with 200 nM Dns-C_6-Ch (Heidmann and Changeux, 1979). [^{3}H]AC5 thus specifically incorporates mainly into the complementary γ and δ subunits of the desensitized nAChR, with 5 to 7% efficiency.

For short mixing times (<1 s), we are most likely to have a mixed population of receptors. In the absence of real-time information on nAChR functional state, we cannot assign the labeling results to an identified sate of the receptor [i.e., incorporation into the resting (R) (monoliganded receptors), active (A), and/or intermediate (I) states]. In such conditions, [^{3}H]AC5 incorporates with a very low efficiency (<1%), mainly into the α and γ subunits. The very low labeling of the δ subunit, compared with the γ subunit, in these transient states of the receptors, can be explained either by a lower affinity of the probe or by a lower labeling efficiency. This further demonstrates the nonequivalent pharmacology between the two sites, even for transient states of the receptor.

For intermediate mixing times (1–300 s), we clearly observe a concomitant increase in the labeling of γ and δ sub-

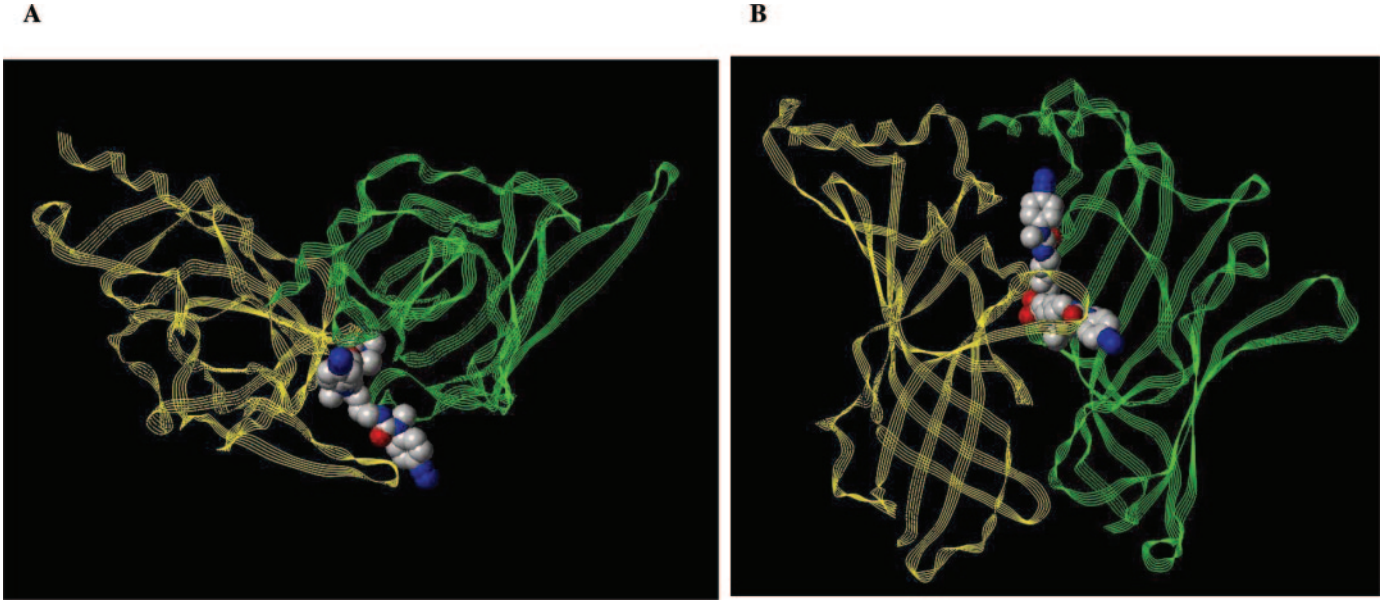

Fig. 5. AC5 probe orientation into an ACh binding site of a presumed resting state-like AChBP structure. The AC5 molecule was docked into an AChBP based on the structure of an AChBP-conotoxin complex, after removing the α-conotoxin. Top (A) and side (B) views of an AChBP dimer (ribbon representation) with two docking results of AC5 molecule (CPK representation), and representative of maximal liberty of the probe in this site.

units (time constant of 0.016 s^{-1}), whereas labeling of the α subunit remains low. This evolution of the labeling very probably represents a structural reorganization of the nAChR toward the D state, because during this process, the labeling yield increases by a factor of 10 to 15. This phenomenon can be associated with an enhancement of AC5 affinity, concomitant on the $\alpha\gamma$ and $\alpha\delta$ binding sites, resulting in a simultaneous occupancy of both binding sites. This increase in the labeling is also compatible with tighter binding sites, resulting in partially dehydrated sites and a higher labeling efficiency. In addition, radioactivity incorporation evolves from a predominant labeling of α and γ subunits to a major labeling of γ and δ subunits. This observation can be explained only in terms of structural reorganization of the ACh binding sites. Finally, the slow relaxation process (half-time ~30 s) observed with Dns-C_6-Ch was assigned to the slow desensitization transition (Heidmann and Changeux, 1979). It is noteworthy that this event can now be explained by the fact that the dansyl fluorophore and the complementary subunit come closer to one another.

AChBP structures in the apo form and in complex with antagonists (Celie et al., 2005; Hansen et al., 2005) recently revealed a more open loop C compared with AChBP in complex with agonists (Celie et al., 2004; Hansen et al., 2005). The fast activation process of the nAChR is thus supposed to require the contribution of only two α subunits (Miyazawa et al., 2003; Law et al., 2005), notably through a movement of loop C, which wraps around the agonist molecule. However, we must keep in mind that conformational states assigned to AChBP crystallized with different ligands are still speculative, and crystallographic structures are not sufficient to describe the complex behavior of nAChR activation and desensitization. Photochemical labeling of the native nAChR thus offers a temporal resolution for such a study. The molecular reorganization we observe here is very slow ($t_{1/2}$ ~ 40 s). Therefore it mostly represents the slow desensitization transition, and cannot be predicted by molecular dynamics simulations, which are limited currently to submicrosecond time scales.

Docking experiments of AC5 into the putative "resting-like" and "desensitized-like" ACh binding sites revealed that a consistent α subunit labeling (mixing time <1 s) can only be explained with a wider ACh binding site, where AC5 has more flexibility (Figs. 4 and 5). The slow reorganization we observe here thus indicates a narrowing of the agonist binding site but probably through a different mechanism than that for the activation. Given the slow kinetics (high activation energy) of this desensitization process, one conceivable model could be a quaternary reorganization of the receptor through the rotation of all five subunits. This rotation would be associated with an enhancement of agonist affinity (Heidmann and Changeux, 1979) and a higher photolabeling efficiency and would position the aromatic part of AC5 closer to the γ and δ subunits. The strong influence of the complementary subunit on the kinetics of desensitization of the nAChRs reinforces this hypothesis of quaternary reorganization during this process (Quick and Lester, 2002). Moreover, recent crystal structures of AChBP revealed for the first time a rigid-body subunit movement for AChBP (Celie et al., 2005; Hansen et al., 2005). AChBP is a water-soluble protein but shares many structural and functional features with the LBD of nAChRs (Sine, 2002; Bouzat et al., 2004). We thus believe that such reorientation of the subunits with respect to one another can be a characteristic of nAChR conformational transitions during desensitization.

Acknowledgments

Many thanks to Johnathan B. Cohen for providing the *T. californica* cDNAs, Marc Nothisen for DNA preparation, and Deniz Dalkara for careful reading of the manuscript.

References

Absalom NL, Lewis TM, Kaplan W, Pierce KD, and Schofield PR (2003) Role of charged residues in coupling ligand binding and channel activation in the extracellular domain of the glycine receptor. *J Biol Chem* **278:**50151–50157.

Bertrand D, Cooper E, Valera S, Rungger D, and Ballivet M (1991) Electrophysiology of neuronal nicotinic acetylcholine receptors expressed in *Xenopus* oocytes following nuclear injection of genes or cDNAs. *Methods Neurosci* **4:**174–193.

Bouzat C, Gumilar F, Spitzmaul G, Wang HL, Rayes D, Hansen SB, Taylor P, and Sine SM (2004) Coupling of agonist binding to channel gating in an ACh-binding protein linked to an ion channel. *Nature (Lond)* **430:**896–900.

Brejc K, van Dijk WJ, Klaassen RV, Schuurmans M, van Der Oost J, Smit AB, and Sixma TK (2001) Crystal structure of an ACh-binding protein reveals the ligand-binding domain of nicotinic receptors. *Nature (Lond)* **411:**269–276.

Case DA, Darden TA, Cheatham TE III, Simmerling CL, Wang RE, Duke RL, Merz ME, Wang DA, Pearlman DA, Crowley M, et al. (2004) AMBER 8, University of California, San Francisco.

Celie PH, Kasheverov IE, Mordvintsev DY, Hogg RC, van Nierop P, van Elk R, van Rossum-Fikkert SE, Zhmak MN, Bertrand D, Tsetlin V, et al. (2005) Crystal structure of nicotinic acetylcholine receptor homolog AChBP in complex with an alpha-conotoxin PnIA variant. *Nat Struct Mol Biol* **12:**582–588.

Celie PH, van Rossum-Fikkert SE, van Dijk WJ, Brejc K, Smit AB, and Sixma TK (2004) Nicotine and carbamylcholine binding to nicotinic acetylcholine receptors as studied in AChBP crystal structures. *Neuron* **41:**907–914.

Changeux JP and Edelstein SJ (1998) Allosteric receptors after 30 years. *Neuron* **21:**959–980.

Chatrenet B, Kotzba-Hibert F, Mulle C, Changeux JP, Goeldner MP, and Hirth C (1992) Photoactivatable agonist of the nicotinic acetylcholine receptor: potential probe to characterize the structural transitions of the acetylcholine binding site in different states of the receptor. *Mol Pharmacol* **41:**1100–1106.

Che C, Petit G, Kotzyba-Hibert F, Bertrand S, Bertrand D, Grutter T, and Goeldner M (2003) Syntheses and biological properties of cysteine-reactive epibatidine derivatives. *Bioorg Med Chem Lett* **13:**1001–1004.

Chiara DC, Trinidad JC, Wang D, Ziebell MR, Sullivan D, and Cohen JB (2003) Identification of amino acids in the nicotinic acetylcholine receptor agonist binding site and ion channel photolabeled by 4-[(3-trifluoromethyl)-3*H*-diazirin-3-yl]benzoylcholine, a novel photoaffinity antagonist. *Biochemistry* **42:**271–283.

Galzi JL, Revah F, Bouet F, Menez A, Goeldner M, Hirth C, and Changeux JP (1991) Allosteric transitions of the acetylcholine receptor probed at the amino acid level with a photolabile cholinergic ligand. *Proc Natl Acad Sci USA* **88:**5051–5055.

Gao F, Bren N, Burghardt TP, Hansen S, Henchman RH, Taylor P, McCammon JA, and Sine SM (2005) Agonist-mediated conformational changes in acetylcholine-binding protein revealed by simulation and intrinsic tryptophan fluorescence. *J Biol Chem* **280:**8443–8451.

Grutter T, Bertrand S, Kotzyba-Hibert F, Bertrand D, and Goeldner M (2002) Structural reorganization of the acetylcholine binding site of the Torpedo nicotinic receptor as revealed by dynamic photoaffinity labeling. *Chembiochem* **3:**652–658.

Grutter T, Prado de Carvalho L, Le Novere N, Corringer PJ, Edelstein S, and Changeux JP (2003) An H-bond between two residues from different loops of the acetylcholine binding site contributes to the activation mechanism of nicotinic receptors. *EMBO (Eur Mol Biol Organ) J* **22:**1990–2003.

Hansen SB, Sulzenbacher G, Huxford T, Marchot P, Taylor P, and Bourne Y (2005) Structures of Aplysia AChBP complexes with nicotinic agonists and antagonists reveal distinctive binding interfaces and conformations. *EMBO (Eur Mol Biol Organ) J* **24:**3635–3646.

Heidmann T and Changeux JP (1979) Fast kinetic studies on the allosteric interactions between acetylcholine receptor and local anesthetic binding sites. *Eur J Biochem* **94:**281–296.

Horenstein J, Wagner DA, Czajkowski C, and Akabas MH (2001) Protein mobility and GABA-induced conformational changes in GABA(A) receptor pore-lining M2 segment. *Nat Neurosci* **4:**477–485.

Jones G, Willett P, Glen RC, Leach AR, and Taylor R (1997) Development and validation of a genetic algorithm for flexible docking. *J Mol Biol* **267:**727–748.

Kash TL, Jenkins A, Kelley JC, Trudell JR, and Harrison NL (2003) Coupling of agonist binding to channel gating in the GABA(A) receptor. *Nature (Lond)* **421:**272–275.

Langenbuch-Cachat J, Bon C, Mulle C, Goeldner M, Hirth C, and Changeux JP (1988) Photoaffinity labeling of the acetylcholine binding sites on the nicotinic receptor by an aryldiazonium derivative. *Biochemistry* **27:**2337–2345.

Law RJ, Henchman RH, and McCammon JA (2005) A gating mechanism proposed from a simulation of a human {alpha}7 nicotinic acetylcholine receptor. *Proc Natl Acad Sci USA* **102:**6813–6818.

Le Novere N, Grutter T, and Changeux JP (2002) Models of the extracellular domain of the nicotinic receptors and of agonist- and Ca^{2+}-binding sites. *Proc Natl Acad Sci USA* **99:**3210–3215.

Lester HA, Dibas MI, Dahan DS, Leite JF, and Dougherty DA (2004) Cys-loop receptors: new twists and turns. *Trends Neurosci* **27:**329–336.

Martinez KL, Corringer PJ, Edelstein SJ, and Changeux JP (2000) Structural

differences in the two agonist binding sites of the Torpedo nicotinic acetylcholine receptor revealed by time-resolved fluorescence spectroscopy. *Biochemistry* **39:** 6979–6990.

Middleton RE and Cohen JB (1991) Mapping of the acetylcholine binding site of the nicotinic acetylcholine receptor: [^{3}H]nicotine as an agonist photoaffinity label. *Biochemistry* **30:**6987–6997.

Miyazawa A, Fujiyoshi Y, and Unwin N (2003) Structure and gating mechanism of the acetylcholine receptor pore. *Nature (Lond)* **423:**949–955.

Molles BE, Tsigelny I, Nguyen PD, Gao SX, Sine SM, and Taylor P (2002) Residues in the epsilon subunit of the nicotinic acetylcholine receptor interact to confer selectivity of waglerin-1 for the alpha-epsilon subunit interface site. *Biochemistry* **41:**7895–7906.

Mourot A, Kotzyba-Hibert F, Doris E, and Goeldner M (2002) New and convenient synthesis of a tritiated photo activatable nicotinic agonist: [H-3]-AC5. *J Labelled Comp Radiopharm* **45:**943–953.

Neubig RR and Cohen JB (1979) Equilibrium binding of [3H]tubocurarine and [^{3}H]acetylcholine by Torpedo postsynaptic membranes: stoichiometry and ligand interactions. *Biochemistry* **18:**5464–5475.

Pedersen SE and Cohen JB (1990) d-Tubocurarine binding sites are located at alpha-gamma and alpha-delta subunit interfaces of the nicotinic acetylcholine receptor. *Proc Natl Acad Sci USA* **87:**2785–2789.

Quick MW and Lester RA (2002) Desensitization of neuronal nicotinic receptors. *J Neurobiol* **53:**457–478.

Schapira M, Abagyan R, and Totrov M (2002) Structural model of nicotinic acetylcholine receptor isotypes bound to acetylcholine and nicotine. *BMC Struct Biol* **2:**1.

Sine SM (2002) The nicotinic receptor ligand binding domain. *J Neurobiol* **53:**431–446.

Song XZ, Andreeva IE, and Pedersen SE (2003) Site-selective agonist binding to the nicotinic acetylcholine receptor from *Torpedo californica*. *Biochemistry* **42:**4197–4207.

Unwin N (2005) Refined structure of the nicotinic acetylcholine receptor at 4A resolution. *J Mol Biol* **346:**967–989.

Unwin N, Miyazawa A, Li J, and Fujiyoshi Y (2002) Activation of the nicotinic acetylcholine receptor involves a switch in conformation of the alpha subunits. *J Mol Biol* **319:**1165–1176.

Wagner DA and Czajkowski C (2001) Structure and dynamics of the GABA binding pocket: A narrowing cleft that constricts during activation. *J Neurosci* **21:**67–74.

Wang D, Chiara DC, Xie Y, and Cohen JB (2000) Probing the structure of the nicotinic acetylcholine receptor with 4-benzoylbenzoylcholine, a novel photoaffinity competitive antagonist. *J Biol Chem* **275:**28666–28674.

Wilson G and Karlin A (2001) Acetylcholine receptor channel structure in the resting, open and desensitized states probed with the substituted-cysteine-accessibility method. *Proc Natl Acad Sci USA* **98:**1241–1248.

Address correspondence to: Dr. Alexandre Mourot, Max Planck Institut für Biophysik, Max-von-Laue str.3, 60 438 Frankfurt am Main, Germany. E-mail: alexandre.mourot@mpibp-frankfurt.mpg.de